

# Dihydroazulene/Vinylheptafulvene Photochromism: Effects of Substituents, Solvent, and Temperature in the Photorearrangement of Dihydroazulenes to Vinylheptafulvenes

Helmut Görner,<sup>\*1</sup> Christian Fischer,<sup>2</sup> Sebastian Gierisch,<sup>2</sup> and Jörg Daub<sup>2</sup>

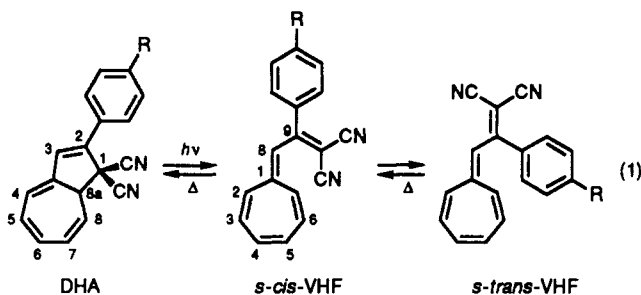
Max-Planck-Institut für Strahlenchemie, D-4330 Mülheim an der Ruhr, Germany, and Institut für Organische Chemie der Universität Regensburg, D-8400 Regensburg, Germany

Received: January 8, 1993

1,1-Dicyano-2-phenyl-1,8a-dihydroazulene (H-D) and a series of *p*-phenyl-substituted derivatives (R-D, R: NO<sub>2</sub>, CN, Br, Cl, CH<sub>3</sub>, OCH<sub>3</sub>, and NH<sub>2</sub>) were investigated by time-resolved and steady-state photochemical methods. The dihydroazulenes (DHAs) undergo an efficient photoreaction to the corresponding vinylheptafulvenes (VHFs), the quantum yield ( $\Phi_{D \rightarrow V}$ ) at room temperature ranges from 0.1 to 0.6. The VHFs ( $\lambda_V = 440\text{--}470$  nm) are nonemitting and photochemically nonreactive and undergo a thermal rearrangement. The activation energy for this back-reaction is 18–21 kcal/mol. The *A* factor is in the  $(0.01\text{--}5) \times 10^{10} \text{ s}^{-1}$  range; it varies with substituent and increases with increasing solvent polarity. The photoproduct is formed via a singlet pathway,  $^1\text{DHA}^* \rightarrow \text{VHF}$ ; triplet states are not involved in this reaction. Fluorescence from the DHAs was observed, weakly in fluid solution and most efficiently in glasses at low temperatures (e.g.,  $\lambda_f \approx 480$  nm for the parent compound). The quantum yield ( $\Phi_f$ ) at  $-196$  °C ranges from 0.15 to 0.9. A transient ( $\lambda_{\text{max}} \approx 450$  nm,  $\tau_T \leq 5$   $\mu\text{s}$ ), detectable at room temperature only on excitation of a sensitizer (e.g., xanthone in acetonitrile), is assigned to the lowest DHA triplet. In viscous media, where  $\Phi_{D \rightarrow V}$  is strongly retarded, the triplet is observable on direct excitation with a lifetime of less than 10  $\mu\text{s}$  even at  $-196$  °C. The increase of  $\Phi_f$  and the reverse effect for  $\Phi_{D \rightarrow V}$  with decreasing temperature indicates competition of these processes due to an activation barrier (<5 kcal/mol) along the  $^1\text{DHA}^* \rightarrow \text{VHF}$  pathway. Characteristic features of the ground-state and first excited singlet energy surfaces are presented.

## Introduction

Organic compounds with photochromic properties are receiving considerable attention because of possible applications for processing of information.<sup>3–6</sup> Numerous structural entities exhibiting photochromism were developed and investigated.<sup>4</sup> The system dihydroazulene (DHA)/vinylheptafulvene (VHF) constitutes a new class of photochromic couple with powerful potential.<sup>5–7</sup>



In previous studies the scope of the physical and chemical properties of the DHA/VHF system has been evaluated, demonstrating that the primary forward reaction is of photochemical nature and the subsequent back-reaction occurs thermally.<sup>5–8</sup> In principle, the photoreaction requires an *s-cis*-VHF before the more stable *s-trans* configuration is formed. By X-ray analysis the structure of the photoproduct has been found to be *s-trans*-VHF.<sup>6</sup>

The photochromic DHA/VHF system is of the rare type of a 10- $\pi$ -electron rearrangement and comprises the conversion of an alternant  $\pi$ -system into a carbon skeleton and nonalternant connectivity in VHF.<sup>5–9</sup> Therefore, pronounced effects by substituents, for example, when attached in C-2 in DHA, are expected. Consequently, this has been successfully utilized in molecular switching.<sup>7b</sup> Treatment of a properly substituted DHA with light pulse excitation leads to the triggering of an electrical current, as shown by photomodulation amperometry.<sup>7a,8</sup>

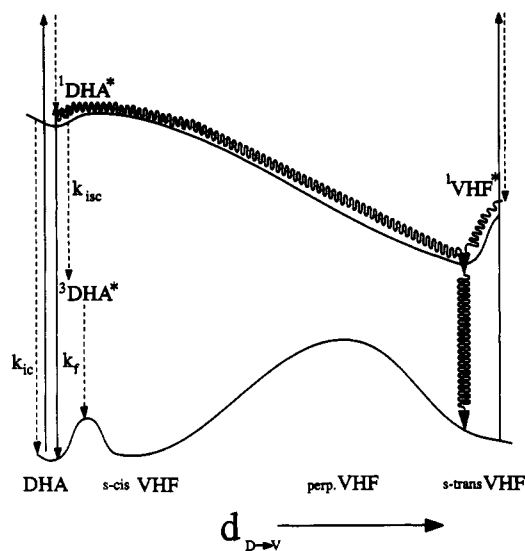
This paper deals with 1,1-dicyano-2-phenyl-1,8a-dihydroazulene (H-D) and seven *p*-phenyl-substituted derivatives (NO<sub>2</sub>-, CN-, Br-, Cl-, CH<sub>3</sub>-, OCH<sub>3</sub>-, and NH<sub>2</sub>-D). We are now extending the previous studies on a broader basis in order to characterize the effects quantitatively and to gain a better understanding of the photophysical, kinetic, and thermodynamic parameters and aspects. Time-resolved and steady-state photochemical techniques are employed for elucidating the photochemical reaction pathways. The energetics of the forward and back reactions are illustrated in Scheme I. Briefly, we suggest (i) a maximum in the ground-state surface between *s-cis*- and *s-trans*-VHF and (ii) a minimum in the excited singlet state surface at a geometry close to the *s-trans*-VHF configuration.

## Experimental Section

Synthesis of the parent molecule, 1,1-dicyano-2-(4-R-phenyl)-1,8a-dihydroazulene (H-D) and the phenyl-substituted derivatives, where R is NO<sub>2</sub>, Br, CH<sub>3</sub>, OCH<sub>3</sub>, and NH<sub>2</sub> (denoted as R-Ds), have been described elsewhere.<sup>5,6</sup> The molar extinction coefficients of DHAs are in the range of  $(1.2\text{--}2.8) \times 10^4 \text{ M}^{-1} \text{ cm}^{-1}$ , and those of the VHFs are generally somewhat larger.<sup>6,7f</sup> Details for synthesis of Cl-D and CN-D are given in refs 7e and 7f, respectively. The solvents (Merck or Fluka) were analytical quality glycerol triacetate (GT) or Uvasol quality acetonitrile; methylcyclohexane (MCH) was purified by passing it through a basic alumina column (Woelm); toluene, 2-methyltetrahydrofuran (MTHF), butyronitrile, and ethanol were distilled.

Steady-state measurements were performed using an absorption spectrophotometer (Perkin-Elmer, 554) and two spectrofluorimeters (Perkin-Elmer, LS-5 and a Spex-Fluorolog); the latter was used for corrected spectra, and the former could also be used for time-resolved spectra, e.g. to separate fluorescence from possible phosphorescence.<sup>10,11</sup> The quantum yield of fluorescence was obtained using 9,10-diphenylanthracene in ethanol as reference ( $\Phi_f = 1.0$  at  $-196$  °C).<sup>12</sup> The absorbances (*A*) were kept below 0.4 per 1-cm pathlength; no corrections were made

**SCHEME I. Accounting for the DHA → VHF Photoconversion and the Absence of the Photochemical Back-Reaction**



for the refractive index of the solvents and the temperature dependent changes in absorbance at  $\lambda_{exc}$ . Fluorescence decay kinetics were measured with a single-photon counting apparatus.<sup>10</sup> This technique proved to be useful only in rigid glasses due to the apparatus time resolution of  $\approx 0.6$  ns and the too small  $\Phi_f$  values at room temperature.

Continuous irradiation was carried out using a 1000-W Hg-Xe lamp combined with a monochromator. The relative  $\Phi_{D \rightarrow V}$  values were obtained from the initial linear dependences of the absorption changes at the maximum of the VHF's ( $\lambda_V$ ) vs the number of absorbed photons using absorbances of  $\approx 2$  (per 1 cm) at  $\lambda_{irr} = 366$  nm. The absolute quantum yield was obtained by using ferrioxalate as actinometer.<sup>13</sup> Standard low-temperature measurements were carried out in appropriate Dewars; for measurements of the photoreaction the samples were subsequently warmed and the absorption spectra were then recorded at room temperature throughout. The rate constant for the thermal back-reaction was obtained from the absorption changes at  $\lambda_V$  at a fixed temperature, monitored by a thermocouple.

Laser flash photolysis with a time resolution of 15–20 ns was carried out as described previously;<sup>10,11c</sup> the wavelengths of excitation (353 and 248 nm) were provided by a neodymium laser (pulse width 15 ns) and a KrF excimer laser, respectively. The DHA concentrations for the sensitized measurements were much larger than those (typically 0.05–0.5 mM) for direct excitation due to the requirement of sufficient quenching of the donor triplet. In order to suppress the DHA → VHF photoreaction, the concentration of the donor used was as large as possible (corresponding to  $A_{248} = 3$  per 1-mm pathlength) without hindering optical detection.

## Results

**Emission Properties.** For the eight compounds in several solvents of different polarity, e.g., MCH, MTHF, butyronitrile, or ethanol, at room temperature, only weak emission could be detected (if at all) using  $\lambda_{exc} = 366$  nm (Table I). Examples of the emission spectra in ethanol at 24 °C are shown in Figure 1a and b for CN-*D* and NH<sub>2</sub>-*D*, respectively. The respective maxima ( $\lambda_f$ ) are located at 448 and 500 nm. The emission intensity increases strongly when the temperature is decreased to –196 °C, e.g., by a factor of  $\approx 900$  for CN-*D* in ethanol. Therefore, in all cases examined, the emission could be detected in glassy media with a much better accuracy. The emission is ascribed to fluorescence due to its decay kinetics.

The fluorescence lifetime ( $\tau_f$ ) for the DHAs in glassy media was obtained from monoexponential fitting of the single-photon counting decay curves ( $\lambda_{exc} = 354$  nm); in some cases a simulation with two lifetimes, e.g., 0.6- and 3.8-ns components for H-*D* in ethanol at –196 °C, gave a better fit ( $X^2$  values). Nevertheless, only the main (longer-lived) component is presented here, when the other component contributes less than 20% of the total decay. Typical  $\tau_f$  values are in the 2–4 ns range, e.g., 3.4 and 3.6 ns for CN-*D* in ethanol and butyronitrile, respectively.

For a given compound  $\lambda_f$  is red-shifted, typically by about 30 nm, on going from 24 to –196 °C. The fluorescence of the DHAs in glassy solvents at –196 °C exhibits one band with  $\lambda_f = 474$ –530 nm, depending on substitution (Table I). No phosphorescence could be detected at –196 °C on a longer time scale, e.g., 20  $\mu$ s after the exciting flash. Solvent properties, e.g., the strongly increasing polarity in the order MCH, MTHF, butyronitrile, and ethanol, have only a small influence on  $\lambda_f$ . The largest effect on  $\lambda_f$ , a red shift of up to 50 nm at –196 °C, arises from variation of the substituent, on going from H-*D* to OCH<sub>3</sub>- and NH<sub>2</sub>-*D*. Examples of the fluorescence emission spectra together with the excitation spectra are shown in Figure 1. The similarity between the excitation spectrum (maximum;  $\lambda_f^{ex}$ ) and the absorption spectrum supports the conclusion that the fluorescence arises from the <sup>1</sup>DHA\* state.

In glassy media at –196 °C, the  $\lambda_f^{ex}$  values are generally displaced to longer wavelengths compared to those at 24 °C. Such small red-shifts of the absorption maximum and  $\lambda_f^{ex}$  may be considered as a typical effect of temperature. Moreover, on decreasing the temperature  $\lambda_f$  is first red-shifted to a maximum value at about –150 °C and then slightly blue-shifted (results not shown).

In some cases, e.g., for H-*D* and CN-*D* in glassy ethanol, it was tested whether or not the photoproduct also shows an emission. The fluorescence spectrum at –196 °C, after sufficient DHA → VHF conversion (>50%) at ambient temperatures, does not change, apart from an effect due to absorption of the DHA fluorescence by the VHF photoproduct in the 450–550-nm range. On the other hand, the fluorescence intensity (at  $\lambda_f$  and –196 °C) decreases in proportion to the conversion of a given DHA into the VHF, when irradiated beforehand at 24 °C. Moreover, no new emission appeared on selective excitation of VHF, e.g.,  $\lambda_{exc} = 450$  nm. From this we conclude that the excited VHF state does not emit.

**Quantum Yield of Fluorescence.** The fluorescence quantum yield ( $\Phi_f$ ) of the DHAs in glassy media is substantial; typical values are  $\Phi_f = 0.5$ –0.9 (Table I).  $\Phi_f$  is essentially independent of the solvent properties, e.g. polarity, and variation of  $\lambda_{exc}$  between 300 and 400 nm has no pronounced effect. Smaller  $\Phi_f$  values of 0.15–0.4 were only obtained for OCH<sub>3</sub>-*D* and NH<sub>2</sub>-*D*. For CN-*D* in ethanol at –196 °C it was found that the absence or presence of oxygen has no effect on  $\Phi_f$ .

When the temperature is increased,  $\Phi_f$  decreases slightly in the range below about –150 °C, where the solvents are typically highly viscous,<sup>14</sup> and decreases steeply at higher temperatures (Figures 2 and 3). The changes in  $\Phi_f$  between –196 and 24 °C are largest, more than 3 orders of magnitude for H-*D* and CN-*D* and smaller for NH<sub>2</sub>-*D* (Table II). The solvent also has some influence on these changes. The largest  $\Phi_f$  value at room temperature was obtained for NH<sub>2</sub>-*D* in MTHF, a solvent of medium polarity.

Semilogarithmic plots of  $\Phi_f$  on  $T^{-1}$  show an Arrhenius behavior in the cases examined. Examples are presented in Figure 2 for parent H-*D* in ethanol and GT (glycerol triacetate) and in Figure 3 for CN-*D* and NH<sub>2</sub>-*D* in ethanol. A typical activation energy is 3 kcal/mol, e.g., for H-*D* or CN-*D* in several solvents, except for GT, where the curves of  $\log \Phi_f$  vs  $T^{-1}$  are usually steeper due to the additional effect of viscosity.

**TABLE I: Maxima of Fluorescence Excitation and Emission Spectra of DHAs and Quantum Yield of Fluorescence<sup>a</sup>**

substit	solvent	at 24 °C			at -196 °C		
		$\lambda_f^{ex}$ , nm	$\lambda_f$ , nm	$\Phi_f$	$\lambda_f^{ex}$ , nm	$\lambda_f$ , nm	$\Phi_f$
NO <sub>2</sub>	ethanol			<0.001	363	474	0.8
CN	MTHF	355	445	0.0003	381	479	0.8
	butyronitrile	357	448	0.001	377	478	0.8
Br	ethanol	355	448	0.001	378	480	0.9
	MTHF	360	442	0.001	367	476	0.5
Cl	ethanol				368	480	0.8
	MTHF	360	446	0.001	370	481	0.6
H	ethanol				365	478	0.8
	MCH				360	476	0.9
	MTHF	350	460	$\leq 0.0003$	365	478	0.7
	butyronitrile	350	460	$\leq 0.0003$	362	476	0.8
CH <sub>3</sub>	butyronitrile <sup>b</sup>				477	477	0.9
	ethanol	352	460	0.0003	362	480	0.9
OCH <sub>3</sub>	ethanol	353	460	$\leq 0.001$	365	498	0.8
	MTHF	365	450	0.003	376	497	0.4
NH <sub>2</sub>	butyronitrile				372	496	0.4
	ethanol	370	475	$\leq 0.001$	374	500	0.4
	MTHF	370	480	0.005	410	527	0.2
	butyronitrile	372	480	0.002	402	524	0.25
	ethanol	370	500	0.0014	404	530	0.15

<sup>a</sup>  $\lambda_f = 480\text{--}500$  nm for excitation spectra;  $\lambda_{exc} = 366$  nm for emission, unless otherwise indicated. <sup>b</sup>  $\lambda_{exc} = 313$  nm.

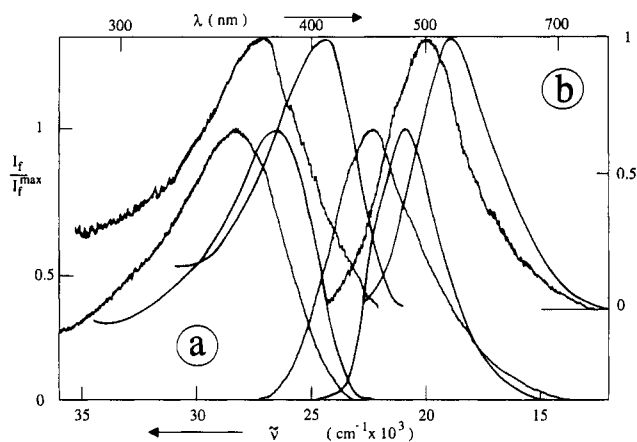


**Figure 1.** Fluorescence excitation and emission spectra in ethanol at 24 °C (left) and -196 °C (right) for (a) CN-*D* and (b) NH<sub>2</sub>-*D*;  $\lambda_{exc} = 366$  nm,  $\lambda_f \approx 500$  nm.

A close correlation between  $\Phi_f$  and  $\tau_f$  values, as often found for more straightforward cases,<sup>15</sup> was not detected for the DHAs in glasses at -196 °C. For example, the decrease in  $\Phi_f$  in several solvents on going from CN-*D* ( $\approx 0.9$ ) to NH<sub>2</sub>-*D* (0.15–0.25) is not reflected by a corresponding decrease in  $\tau_f$ ; in ethanol these values are 3.2 and 2.9 ns, respectively. From the changes in  $\Phi_f$  between 24 and -196 °C,  $\tau_f$  values of the order of 10 ps are expected in solution at room temperature, when no marked effect on the rate constant of the radiative transition is assumed.

**Photochemical Reaction of DHAs to VHF.** Irradiation (at 366 nm) of DHAs in various solvents at room temperature reveals the formation of a single photoproduct which has previously been identified as the corresponding *s-trans*-VHF isomer.<sup>5–7</sup> Two examples are shown in Figures 4 and 5 for parent H-*D* and NH<sub>2</sub>-*D* in acetonitrile, respectively. Because of this clean photoreaction several isosbestic points become apparent. Two of them, ranging from 288 nm for NH<sub>2</sub>-*D* in acetonitrile to 314 nm for CN-*D* in ethanol and from 382 nm for H-*D* in MCH to 407 nm for CN-*D* in ethanol, mark the bleaching area. Two related characteristic wavelengths,  $\lambda_D$  and  $\lambda_V$ , the maxima of the DHA and VHF absorption, respectively, depend only slightly on both the solvent properties and the substituent. Variation of the wavelength of irradiation (254–405 nm) has virtually no effect on the absorption spectra. A significant blue-shift for both  $\lambda_D$  and  $\lambda_V$  occurs for several cases when a polar solvent or toluene, which is slightly polar, are replaced by the nonpolar MCH. For NH<sub>2</sub>-*D*, by

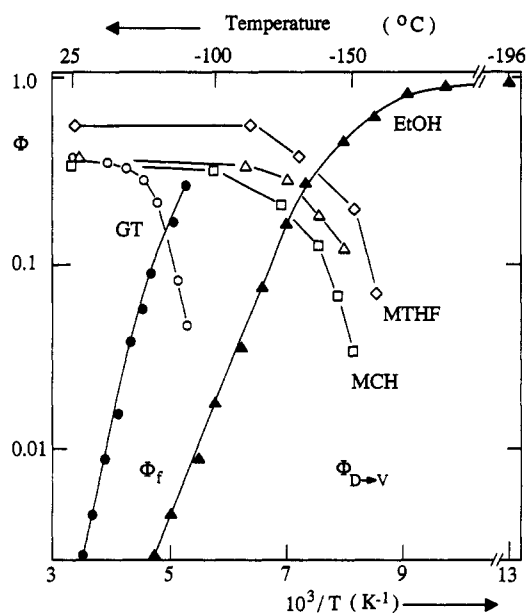


**Figure 2.** Temperature dependence of  $\log \Phi_f$  (full symbols) and  $\log \Phi_{D \rightarrow V}$  (open symbols) for H-*D* in MCH ( $\square$ ), MTHF ( $\diamond$ ), GT (circles), and ethanol (triangles);  $\lambda_{exc} = 366$  nm.

comparison with other DHAs,  $\lambda_D$  is red-shifted but  $\lambda_V$  blue-shifted, the photochromic shift is therefore smallest for NH<sub>2</sub>-*D*.

All attempts to force a photoreaction from VHF derivatives at ambient temperature, e.g., by variation of the substituent or the solvent, failed. In particular, upon selective irradiation of the VHF isomer of the parent compound in the range 450–600 nm, the absorption spectrum does not change (apart from the thermal back-conversion on a prolonged time scale, vide infra). This strongly suggests that there is no photoreaction from VHF to DHA; i.e., the photochromism is photochemically irreversible.

To test for the possibility of a DHA  $\rightarrow$  VHF pathway via triplet state, several sensitizers, e.g., acetone, acetophenone, and biacetyl, were used. Because of the extension of the absorption spectra of the DHAs up to 400–450 nm, the requirement of a selective excitation into the sensitizer cannot be fulfilled with high-energy sensitizers. When biacetyl in argon-saturated acetonitrile at room temperature was irradiated at 436 nm in the presence of H-*D* (at a concentration of 0.1 mM), indeed the DHA  $\rightarrow$  VHF photoconversion became apparent. However, control experiments showed that this was due only to the small

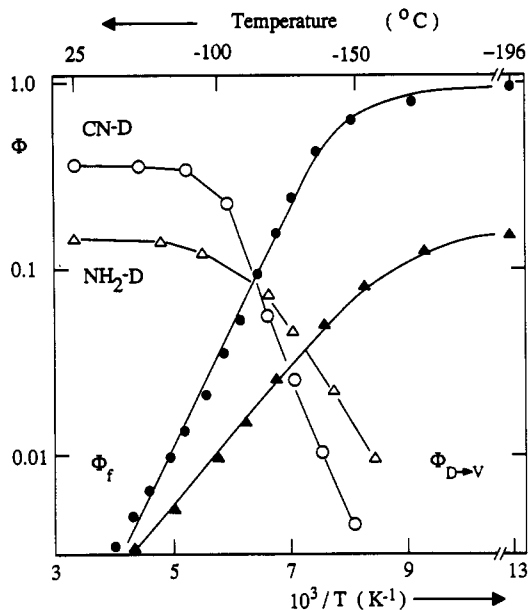


**Figure 3.** Temperature dependence of  $\log \Phi_f$  (full symbols) and  $\log \Phi_{D \rightarrow V}$  (open symbols) for CN-D (circles) and NH<sub>2</sub>-D (triangles) in ethanol;  $\lambda_{exc} = 366$  nm.

**TABLE II: Effects of Temperature on  $\Phi_f$  and  $\Phi_{D \rightarrow V}$  for DHAs<sup>a</sup>**

substit	solvent	temp, °C	$\Phi_f$	$\Phi_{D \rightarrow V}$
CN	MTHF	25	0.0003	0.3
		-100	0.02	0.1
		-150	0.6	0.02
	ethanol	25	0.001	0.35
		-100	0.04	0.2
		-150	0.7	0.004
H	D-P/MCH	25	0.0001	0.35
		-100	0.03	0.32
		-150	0.6	0.032
	MTHF	25	<0.0002	0.58
		-100	0.03	0.52
		-150	0.5	0.06
GT	25	0.002	0.4	
	-100	>0.4	<0.01	
	ethanol	25	<0.0002	0.5
	-100	0.02	0.45	
	-150	0.6	0.1	
	OCH <sub>3</sub>	D-P	25	<0.001
-100			0.03	0.4
ethanol			25	0.0005
	-100	0.05	0.3	
	-150	0.2	0.06	
	NH <sub>2</sub>	ethanol	25	0.0012
-100			0.01	0.13
-150			0.08	0.004

<sup>a</sup>  $\lambda_{irr} = 366$  nm.

fraction of light absorbed by H-D itself. Since the efficiency of VHF formation is not enhanced under sensitized excitation conditions, a triplet route for the direct DHA  $\rightarrow$  VHF photo-reaction is therefore unlikely.

**Effects of Substituents, Solvent, and Temperature on  $\Phi_{D \rightarrow V}$ .** At room temperature the quantum yield of VHF formation ( $\Phi_{D \rightarrow V}$ ) depends to a certain degree on substitution and solvent. The values in acetonitrile range from 0.35 to 0.65 in all cases except for NH<sub>2</sub>-D (Table III and Figure 5). For H-D and CN-D  $\Phi_{D \rightarrow V}$  is smaller in MCH and ethanol than in toluene and acetonitrile, whereas for NH<sub>2</sub>-D  $\Phi_{D \rightarrow V}$  decreases in the order of MCH, toluene, and acetonitrile. For H-D in acetonitrile it was found that changing  $\lambda_{irr}$  from 366 to 313 nm and further to 254 nm has no effect (within experimental error) on  $\Phi_{D \rightarrow V}$ . Effects of O<sub>2</sub> (air- or oxygen-saturation vs argon-saturation) on both the spectra and  $\Phi_{D \rightarrow V}$  were not found.

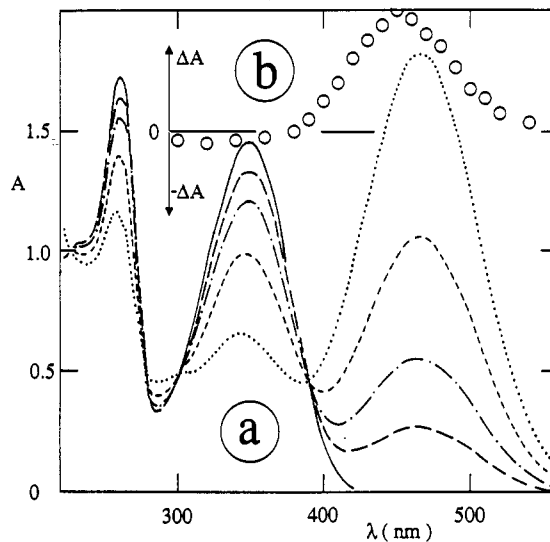


**Figure 4.** (a) Absorption spectra for H-D in acetonitrile at 24 °C prior to (full line) and after irradiation (5, 10, 20, and 40 s;  $\lambda_{irr} = 366$  nm) and (b) transient difference spectrum  $\approx 50$  ns after the pulse;  $\lambda_{exc} = 353$  nm.

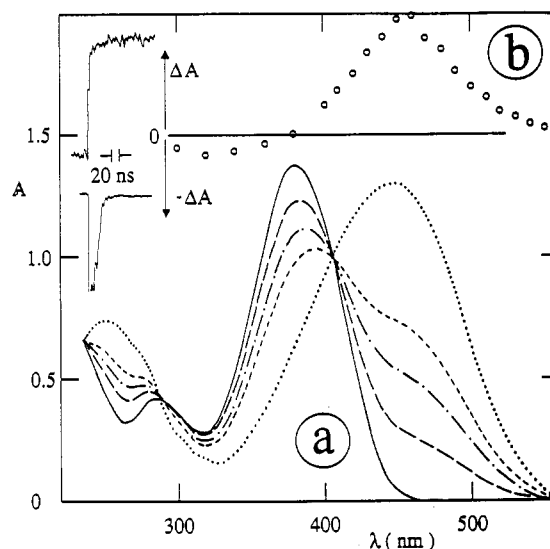


**Figure 5.** (a) Absorption spectra for NH<sub>2</sub>-D in acetonitrile at 24 °C prior to (full line) and after irradiation (20, 40, 60, and 200 s;  $\lambda_{irr} = 366$  nm) and (b) transient difference spectrum  $\approx 50$  ns after the pulse. Insets: time dependence of the product formation at 460 nm (upper) and of the 248-nm laser pulse itself (lower).

Generally, the DHA  $\rightarrow$  VHF photoreaction is efficient even in solution at lower temperatures. In this respect GT is an exception due to its relatively high viscosity in the temperature range 0 to  $-80$  °C.<sup>14</sup> For several DHAs in fluid media there is practically no change in  $\Phi_{D \rightarrow V}$  between 25 and  $-100$  °C (Table II). However, when the temperature is further decreased, e.g., to  $-150$  °C,  $\Phi_{D \rightarrow V}$  decreases significantly. Plots of  $\log \Phi_{D \rightarrow V}$  vs  $T^{-1}$  are shown in Figure 2 for H-D in several solvents and in Figure 3 for CN-D and NH<sub>2</sub>-D in ethanol. The results from irradiation at low temperatures are in agreement with the corresponding curves for  $\Phi_f$ . The main deactivation process is governed by both temperature and viscosity, as is indicated by a comparison of the  $\Phi_{D \rightarrow V}$  and  $\Phi_f$  dependences in either GT or the more fluid media (Figure 2).

**Thermal Reaction of VHF to DHAs.** For several derivatives it has previously been shown that DHA is thermochemically more stable than VHF.<sup>6,7a,b,e,f</sup> Nevertheless, insufficient information is given concerning the thermal back-conversion. We have therefore determined the activation energy ( $E_a$ ) and the pre-exponential factor for various conditions (Table IV). In all cases

**TABLE III: Absorption Maxima of DHA and VHF and Quantum Yield of VHF Formation<sup>a</sup>**

substit	solvent	$\lambda_D$ , nm	$\lambda_V$ , nm	$\Phi_{D \rightarrow V}$
NO <sub>2</sub>	acetonitrile	352	472	0.6
CN	MCH	361	452	0.4
	toluene	368	470	0.65
	acetonitrile	362	474	0.6 <sup>b</sup>
	ethanol	362	474	0.35
Br	acetonitrile	355	474	0.5
	acetonitrile	353	472	0.55
	MCH	349	440	0.35
	toluene	354	459	0.6
H	acetonitrile	350	468	0.55 <sup>b</sup>
	ethanol	348	468	0.5
	MCH	352	440	0.4
	acetonitrile	352	466	0.5
CH <sub>3</sub>	acetonitrile	360	465	0.4
OCH <sub>3</sub>	acetonitrile	376	440	0.4
	toluene	382	448	0.3
NH <sub>2</sub>	acetonitrile	381	450	0.15

<sup>a</sup> In (nondegassed) solutions at 24 °C,  $\lambda_{irr} = 366$  nm. <sup>b</sup> Same value under argon.

**TABLE IV: Activation Energy, A Factor, and Rate Constant at Room Temperature for the Thermal VHF → DHA Reaction<sup>a</sup>**

substit	solvent	$E_a$ , kcal/mol	$A$ , s <sup>-1</sup> × 10 <sup>10</sup>	$k_{V \rightarrow D}(25\text{ °C})$ , s <sup>-1</sup> × 10 <sup>-5</sup>
NO <sub>2</sub>	acetonitrile	19.0	0.6	13
CN	MCH	18	0.01	0.8
	GT	19.1	0.8	12
H	acetonitrile	19.7	3.0	16
	ethanol	19.2	1.5	20
	MCH	20.9	0.16	0.12
	toluene	20.5	0.8	1.2
CH <sub>3</sub>	GT	19	0.3	4.8
	acetonitrile	20.3	3.5	7
	ethanol	19	0.5	9
	MCH	20.8	0.1	0.1
OCH <sub>3</sub>	acetonitrile	20.2	3	7
	acetonitrile	20.6	5	7
NH <sub>2</sub>	acetonitrile	20.0	2	6

<sup>a</sup> Obtained from standard procedures in the 50–100 °C range for (nondegassed) MCH, toluene, and GT and in the 25–70 °C range for acetonitrile and ethanol.

the plots of ln (% conversion) vs time are linear at a fixed temperature. Likewise, for a given compound/solvent combination the semilogarithmic plots of the rate constants ( $k_{V \rightarrow D}$ ) are linearly dependent on  $T^{-1}$ . Examples for the parent compound in several solvents are shown in Figure 6.

The  $E_a$  values depend only slightly on both the medium and substituent. Typical values for the frequency factor in acetonitrile are  $A = (2\text{--}5) \times 10^{10}$  s<sup>-1</sup>; they are markedly smaller only for NO<sub>2</sub>-D. The most pronounced effect is a decrease (by more than 1 order of magnitude) of the  $A$  factor with decreasing solvent polarity, as shown for CN-D and H-D on going from acetonitrile to toluene and further to MCH (Table IV). Thus, a nonpolar solvent is even more suitable for long-time irradiation studies. This thermal back-conversion plays virtually no role for our steady-state measurements at room temperature since a typical rate constant of  $6 \times 10^{-5}$  s<sup>-1</sup> (Table IV) corresponds to a VHF lifetime of about 4 h.

**Laser Flash Photolysis Studies.** Excitation (at 353 nm) of DHAs in fluid solution at room temperature yields an increase in the absorbance at 420–550 nm within the pulse width and a corresponding decrease in the bleaching range between the two isosbestic points, typically between 320 and 380 nm. Examples are shown in Figures 4b and 5b for H-D and NH<sub>2</sub>-D in acetonitrile, respectively. These laser-induced spectral changes are in agreement with formation of the VHF photoproduct within 15 ns. Owing to the high values of  $\Phi_{D \rightarrow V}$  and the molar extinction

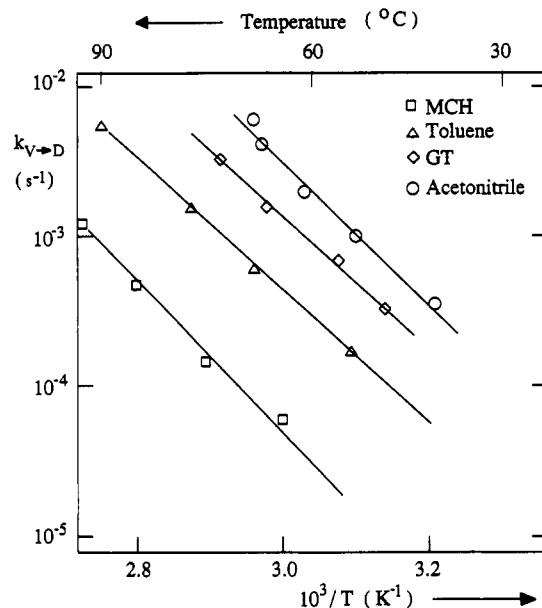


Figure 6. Arrhenius plots for the rate constant of the thermal back-conversion (logarithmic scale) for H-D in MCH (□), toluene (Δ), GT (◇), and acetonitrile (○).

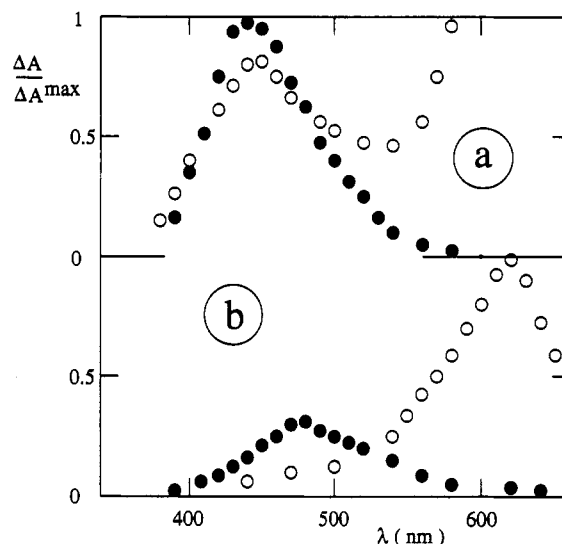


Figure 7. Transient absorption spectra in argon-saturated acetonitrile at 24 °C upon xanthone-sensitized excitation at 20 ns (○) and 0.5 μs (●) after the pulse for (a) H-D and (b) NH<sub>2</sub>-D;  $\lambda_{exc} = 248$  nm.

coefficients (see above), together with the broad absorption spectra of the VHF, any weakly absorbing transient in the 200–550-nm range would hardly be detectable at all.

To gain information about a DHA triplet state, high-energy triplet donors were excited at 248 nm in the presence of DHAs. Since the direct excitation of the DHAs is not accompanied by a transient in a detectable yield, selective excitation of the sensitizer is not necessary. Using xanthone with a triplet energy of 72 kcal/mol, its first-order decay rate constant ( $k_{obs}$ ) in deoxygenated acetonitrile at room temperature, measured at the T–T absorption maximum at 620 nm,<sup>16</sup> increases linearly with the H-D concentration. From this the rate constant ( $k_q$ ) for quenching the xanthone triplet was measured to be about  $1 \times 10^{10}$  M<sup>-1</sup> s<sup>-1</sup>; i.e.,  $k_q$  is close to the diffusion-controlled limit.

The absorption spectrum of the triplet (<sup>3</sup>DHA\*, for assignment see Discussion) of several DHAs could be detected by this method. Examples are shown in Figure 7a and b for H-D and NH<sub>2</sub>-D, respectively. The maximum of the T–T absorption spectrum is in the 450–500-nm range and the triplet lifetime ( $\tau_T$ ) is a few μs (Table V). It should be noted that the spectra of both the triplet

**TABLE V: Absorption Maximum and Lifetime of the Triplet of the DHAs, Obtained on Sensitized Excitation<sup>a</sup>**

substit	sensitizer	$\lambda_{\max}$ , nm	$\tau_T$ , $\mu\text{s}$
CN	xanthone	445	$\approx 4$
H	xanthone <sup>b</sup>	c	
	xanthone	440	$\approx 5$
CH <sub>3</sub>	acetophenone	450	$\leq 3$
	xanthone	450	$\leq 3$
	benzophenone	450	$\leq 3$
	1-nitronaphthalene	450	$\leq 3$
	9,10-dibromoanthracene	$\approx 460$	$\leq 3$
OCH <sub>3</sub>	xanthone	450	$\approx 5$
NH <sub>2</sub>	xanthone	480	$\approx 3$

<sup>a</sup> In argon-saturated acetonitrile at room temperature,  $\lambda_{\text{exc}} = 248$  nm unless indicated otherwise. <sup>b</sup>  $\lambda_{\text{exc}} = 353$  nm. <sup>c</sup> A possible T-T absorption is overlapped by too efficient VHF formation.

**TABLE VI: Maximum and Lifetime of the Transient upon Direct Excitation of DHAs at Low Temperatures<sup>a</sup>**

substit	solvent	temp, °C	$\lambda_{\max}$ , nm	$\tau$ , <sup>b</sup> $\mu\text{s}$
CN	ethanol	-196	445	7
		-140	445	4
Br	ethanol	-196	435	7
		-140	435	4
H	MTHF	-196	440	7
		-140	440	4
	GT	-80	440	8
	ethanol	-196	440	7
		-140	440	4
NH <sub>2</sub>	ethanol	-196	470	6

<sup>a</sup> In argon-saturated solutions,  $\lambda_{\text{exc}} = 353$  nm. <sup>b</sup> First-order decay.

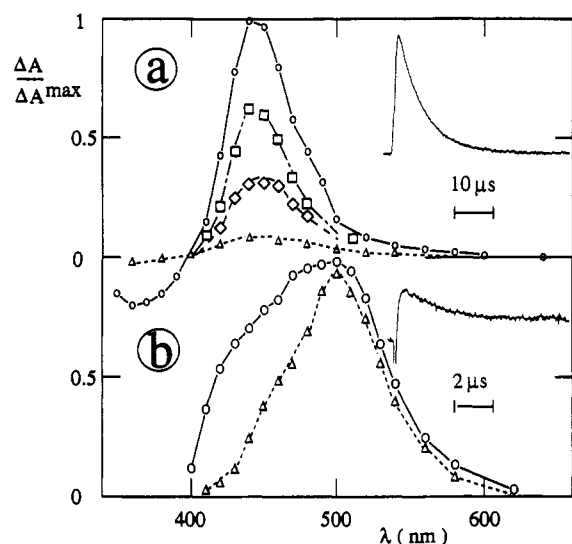


**Figure 8.** Transient absorption spectra for H-D in argon-saturated MTHF at 1 (○), 4 (□), 8 (◇), and 16  $\mu\text{s}$  (Δ) after the pulse at (a)  $-196$  °C and (b)  $-130$  °C. Insets: kinetics at 450 nm,  $\lambda_{\text{exc}} = 353$  nm.

and the VHF-photoproduct are quite similar for each compound. However, the first-order decay of the former and the constant absorbance after laser-induced formation of the latter make a clear distinction possible.

In order to search for spectroscopic information concerning <sup>3</sup>DHA\* on direct excitation, additional low-temperature measurements were carried out ( $\lambda_{\text{exc}} = 353$  nm). Below  $-140$  °C, where  $\Phi_{D \rightarrow V}$  is virtually zero (Table II), a transient with small  $\Delta A$  compared to the efficient photoconversion at room temperature,  $\lambda_{\max}$  around 450 nm, and a lifetime in the 5–8  $\mu\text{s}$  range was recorded for several cases (Table VI). Examples are shown for H-D in MTHF at  $-196$  °C (Figure 8a), i.e., for a condition where the conversion to VHF is frozen out and at  $-130$  °C (Figure 8b), where formation of the "stable" VHF isomer already contributes to the changes in  $\Delta A$ . Assignment of this transient

to <sup>3</sup>DHA\* is based on the similarity of the spectroscopic and kinetic properties (Table V and VI).

Because of the above-mentioned large laser-induced increase in absorption in the 400–450 nm range due to the DHA  $\rightarrow$  VHF photoreaction, a transient, weakly absorbing at 450 nm, cannot be detected under our conditions at temperatures higher than  $-120$  °C in most media (or higher than  $-70$  °C in GT). This renders the usual method for determination of a  $\Phi_{\text{isc}}$  value impossible.

## Discussion

Photochromism as characteristic property of the DHA/VHF system in solution is well documented.<sup>5–7</sup> The DHAs of parent H-D and seven *p*-phenyl-substituted derivatives are photophysically described in terms of the absorption maximum  $\lambda_D = 350$ –380 nm (Table III) and a weak fluorescence at ambient temperature with  $\lambda_f = 442$ –500 nm (Table I). The dominant photochemical process is formation of the *s-trans*-VHF isomer,  $\lambda_V = 440$ –474 nm,  $\Phi_{D \rightarrow V} = 0.15$ –0.65 (Table III). This is a clean reaction, as illustrated by the presence of isosbestic points (Figures 4 and 5) in practically all cases.

The sensitivity of the photochromic couple under examination is regarded to be comparable to (or even to be better than) other systems,<sup>13b</sup> owing to the quite large values of  $\Phi_{D \rightarrow V}$  (Table III) and  $\epsilon_V$ .<sup>6,7e,f</sup> In fact, the product  $\epsilon_V \times \Phi_{D \rightarrow V}$  is of the order of  $1 \times 10^4 \text{ M}^{-1} \text{ cm}^{-1}$  or larger. Fulgides constitute a class of photochromic material, frequently used for actinometric purposes;<sup>13b,17</sup> the sensitivity of Aberchrome 540 is  $1.64 \times 10^3 \text{ M}^{-1} \text{ cm}^{-1}$ , i.e., smaller than for the DHA/VHF system. The ground-state barrier between VHF and DHA (Table IV) is just high enough to allow steady-state measurements at room temperature. Thus, chemical actinometry with DHAs seems promising (nevertheless, more detailed measurements would be desirable).

**Ground-State Properties.** It is well-known that DHA is thermodynamically stable in solution and VHF exists in the solid state as *s-trans* form.<sup>6,7</sup> The back-conversion is characterized by a unique process,  $E_a$  values of  $\approx 20$  kcal/mol,  $A$  factors of the order of  $10^{10} \text{ s}^{-1}$ , and small effects from variation of the substituent (Figure 6 and Table IV). Concerning the potential energy profile of the ground state, two possibilities are envisaged for the position of the activation barrier measured: it is either located between DHA and *s-cis*-VHF or between *s-trans*- and *s-cis*-VHF geometries. The potential energy curve qualitatively described in Scheme I assigns the rate determining step for the thermal back-reaction to *s-trans*-VHF  $\rightarrow$  *s-cis*-VHF isomerization<sup>7e-g,18,19</sup> and takes the mean distance ( $d_{D \rightarrow V}$ ) between position C-1 and C-8a as a parameter to seize the ring opening. From X-ray analysis this bond length has been determined to be 1.568(6) and 1.571(4) Å for Br-D<sup>6</sup> and CN-D<sup>20</sup>, respectively. Data compiled in Table IV reveal that an electron-donating or -accepting substituent at the phenyl ring has virtually no effect on the ground-state energy surface.

**Excited Singlet States.** From the absorption and fluorescence spectra (Table I and Figures 1 and 4) it follows that the energy of the <sup>1</sup>DHA\* state of H-D is about 72 kcal/mol. Variation of the solvent properties and the substituent has a small effect with a trend to a lower level on increasing the electron donating power of R. Estimation of the energy of the <sup>1</sup>VHF\* state is complicated by the total absence of any fluorescence both at either room or low temperatures. This energy is expected to be significantly lower than that of <sup>1</sup>DHA\*. Taking the reciprocal wavelength, at which the absorption at 20% of that at  $\lambda_{\max}$ , as a rough measure for this energy, a value of 53 kcal/mol results for the <sup>1</sup>VHF\* state of H-D. Variation of R would indicate a small increase in the gap for the excited singlet state of the photoproduct on going from VHF to the NH<sub>2</sub>-substituted one (Figures 4 and 5). This effect of substitution is opposite to that for the energy level of <sup>1</sup>DHA\*, where the gap is smallest for NH<sub>2</sub>-D.

When the photoconversion is strongly retarded, e.g., in a rigid glass at  $-196\text{ }^{\circ}\text{C}$ , the dominant step for deactivation of  ${}^1\text{DHA}^*$  is fluorescence,  $\lambda_f = 474\text{--}530\text{ nm}$ . Fluorescence, at least for the cases with  $\text{R} = \text{NO}_2, \text{CN}, \text{Br}, \text{Cl}, \text{H},$  and  $\text{CH}_3$ , accounts for more than 50% of the absorbed photons (Table I). The radiationless modes, being more important in the two remaining cases ( $\text{R} = \text{OCH}_3$  and  $\text{NH}_2$ ), are both weak intersystem crossing ( $k_{\text{isc}}$ ) and internal conversion ( $k_{\text{ic}}$ ), and their relative contribution remains open.

**DHA Triplet State.** Information about a triplet state of the DHA/VHF couple was not available so far.<sup>5-7</sup> The existence of the  ${}^3\text{DHA}^*$  state is based on results from laser flash photolysis (i) at room temperature in the presence of a sensitizer (Figure 7 and Table V) and (ii) at low temperatures in the absence of additives (Figure 8 and Table VI). With xanthone and several other sensitizers we found that a transient remained after the decay of the sensitizer triplet ( ${}^3\text{S}^*$ ), when the DHA concentration was large enough to quench  ${}^3\text{S}^*$  sufficiently. Electron transfer as quenching mechanism is excluded since the same transient was observed with a series of sensitizers having different redox properties. Therefore, energy transfer from  ${}^3\text{S}^*$  to a given DHA (eq 2) accounts for the results, and the transient is assigned to



the DHA triplet state. An alternate assignment to the triplet state of *s-cis*-VHF cannot be totally excluded, but this is regarded to be unlikely since then  ${}^3\text{DHA}^*$  would be the short-lived precursor of the transient. The same has to be anticipated if the observed transient would be assigned to the *s-cis*-VHF ground state. Due to the postulated barrier between the *s-cis*-VHF and DHA ground states, the transient lifetime should reveal a drastic temperature dependence between 25 and  $-196\text{ }^{\circ}\text{C}$ . This, however, is not the case (Tables V and VI).

In order to comment on the possible role of a triplet state in a photoreaction, a knowledge of  $\Phi_{\text{isc}}$  is usually necessary. The  $\Phi_{\text{isc}}$  values are probably low for all DHAs examined and not measurable with the means at our disposal (see Results). Nonetheless, a pathway via the triplet in the  $\text{DHA} \rightarrow \text{VHF}$  reaction is ruled out because the VHF's are completely formed within 50 ns (Figures 4b and 5b); i.e., the conversion is finished, whereas the triplet lifetimes are in the  $\mu\text{s}$  range for the compounds examined (Table V). An estimation of the triplet energy by phosphorescence in glasses at  $-196\text{ }^{\circ}\text{C}$  failed. This is not surprising since such measurements require, besides an efficient radiative transition, substantial  $\Phi_{\text{isc}}$  and sufficiently long  $\tau_T$  values. For the DHAs, however,  $\tau_T$  is very short (Table VI) when one considers that phosphorescence lifetimes of aromatic compounds are typically in the ms-s range.<sup>15</sup>

**Effect of Environment on the Deactivation of  ${}^1\text{DHA}^*$ .** From the very small  $\Phi_f$  and substantial  $\Phi_{\text{D}\rightarrow\text{V}}$  values at room temperature it is clear that, for most DHAs examined, the dominant deactivation process leads to VHF. This should occur in the excited singlet manifold since the triplet route is excluded (see above) and a  $\text{DHA} \rightarrow \text{VHF}$  reaction in the ground state is not possible. In glassy media the contribution of the two modes is reversed;  $\Phi_{\text{D}\rightarrow\text{V}}$  is virtually zero whereas  $\Phi_f$  is substantial or even close to unity (Tables I and II). The temperature dependences of  $\Phi_f$  and  $\Phi_{\text{D}\rightarrow\text{V}}$  (see Figures 2 and 3) suggest that fluorescence and VHF formation are competing processes and that the observed activation barrier lies on the  ${}^1\text{DHA}^* \rightarrow \text{VHF}$  pathway. This barrier is proposed to be composed of two components, one being due to the effect of temperature and an additional viscosity-induced contribution.

On the basis of the processes discussed above, the potential energy profiles of the lowest excited singlet-state surfaces (Scheme I) may qualitatively be described as follows. The curve decreases with increasing reaction coordinate  $d_{\text{D}\rightarrow\text{V}}$ , reaching a minimum

at a configuration which is closer to the *s-trans* than the perpendicular VHF form; i.e.,  $d$  is larger than that corresponding to the maximum between the *s-cis*- and *s-trans*-VHF ground-state geometries. This explains the absence of any measurable photoreaction from the VHF's; i.e., the DHA/VHF couple is photochemically a "one-way" system. A rather small  $\text{S}_1\text{--}\text{S}_0$  gap at the minimum configuration presumably gives rise to rapid internal conversion. Only in this respect does VHF seem to be related to *cis*-olefins, e.g., *cis*-stilbene, and aniles, cf. ref 18. The absence of any detectable fluorescence from the VHF's may indicate that a "free rotor" effect<sup>21</sup> of the exocyclic double bond is responsible for a fast radiationless deactivation.

The result that the sum  $\Phi_f + \Phi_{\text{D}\rightarrow\text{V}}$  is smaller than unity at ambient temperatures, especially in the case of  $\text{NH}_2\text{-D}$  (Table III), is explained by the assumption of internal conversion at geometries between DHA and the perpendicular VHF. The alternative would be internal conversion at the perpendicular VHF configuration and a branching into *s-trans* and *s-cis*, e.g., with a ratio of 40:60, taking a typical  $\Phi_{\text{D}\rightarrow\text{V}}$  value of 0.6. We conclude, however, that this is unlikely since otherwise excitation of *s-trans*-VHF should lead partly to DHA, for which there is no experimental evidence. An increasing contribution of internal conversion at geometries close to DHA could account for smaller  $\Phi_{\text{D}\rightarrow\text{V}}$  values in some cases.

**Effect of Substituent on the Deactivation of  ${}^1\text{DHA}^*$ .** As driving force for the rapid  ${}^1\text{DHA}^* \rightarrow$  perpendicular  ${}^1\text{VHF}^*$  conversion (compared to fluorescence at DHA), we envisage a charge transfer (CT) process upon excitation of DHA. The negative charge is partially localized at the cyano groups and the positive charge at the seven-membered ring. Twisting, going along with intramolecular CT (involving the cyano group) is a well-known phenomenon.<sup>22,23</sup> Such a CT for DHAs may initiate the ring opening, when assisted by the strain of the five-membered ring. Mesomeric forms with CT content are conceivable for *s-trans*-VHF.<sup>6</sup>

This proposal is in agreement with the decrease in  $\Phi_{\text{D}\rightarrow\text{V}}$  in the order  $\text{H-}, \text{OCH}_3\text{-},$  and  $\text{NH}_2\text{-D}$ , e.g., in acetonitrile (Table III). Owing to the electron-donating power of the amino group in  $\text{NH}_2\text{-D}$ , the charge separation between the seven-membered ring and the two cyano groups is suggested to be retarded. Thus, the ring-opening reaction should be slowed down, and in fact  $\Phi_{\text{D}\rightarrow\text{V}}$  is smallest for  $\text{NH}_2\text{-D}$ . On the other hand, the third cyano group in  $\text{CN-D}$  or the nitro group in  $\text{NO}_2\text{-D}$  have obviously no enhancing effect on  $\Phi_{\text{D}\rightarrow\text{V}}$ . This is not surprising taking into account that  $\Phi_{\text{D}\rightarrow\text{V}} = 0.35\text{--}0.6$  even in the absence of an electron-withdrawing substituent.

**Acknowledgment.** We thank Professor D. Schulte-Frohlinde for his support and Mrs. M. Feuerer, E. Hüttel, A. Keil, and S. Roos, Mr. L. J. Currell, and S. Neumann for technical help. C.F. thanks the Fonds der Chemischen Industrie (Frankfurt am Main) for a dissertation fellowship.

## References and Notes

- (1) Max-Planck-Institut für Strahlenchemie.
- (2) Institut für Organische Chemie der Universität Regensburg.
- (3) (a) Dessauer, R.; Paris, J. P. In *Advances in Photochemistry*; Noyes, W. A., Hammond, G. S., Pitts, J. N., Eds.; Interscience: New York, 1963; Vol. 1, p 275. (b) Brown, G. H., Ed. *Photochromism*; Techniques of Chemistry; Wiley Interscience: New York, 1971; Vol. 3. (c) Dürr, H. *Angew. Chem.* **1989**, *101*, 427. (d) Dürr, H. *Pure Appl. Chem.* **1990**, *62*, 1477. (e) Parthenopoulos, D. A.; Rentzepis, P. M. *Science* **1989**, *245*, 843. (f) El'tsov, A. V., Ed. *Organic Photochromes*; Consultants Bureau: New York, 1990.
- (4) Dürr, H.; Bouas-Laurent, H., Eds. *Photochromism—Molecules and Systems*; Studies in Organic Chemistry, 40; Elsevier: Amsterdam, 1990.
- (5) Daub, J.; Knöchel, T.; Mannschreck, A. *Angew. Chem., Int. Ed. Engl.* **1984**, *23*, 960.
- (6) Daub, J.; Gierisch, S.; Klement, U.; Knöchel, T.; Maas, G.; Seitz, U. *Chem. Ber.* **1986**, *119*, 2631.
- (7) (a) Gierisch, S.; Daub, J. *Chem. Ber.* **1989**, *122*, 69. (b) Gierisch, S.; Bauer, W.; Burgemeister, T.; Daub, J. *Chem. Ber.* **1989**, *122*, 2341. (c) Bross, P. A.; Mirlach, A.; Salbeck, J.; Daub, J. *DECHEMA-Monogr.* **1990**, *121*, 375. (d) Daub, J.; Gierisch, S.; Salbeck, J. *Tetrahedron Lett.* **1990**, *31*,

3113. (e) Gierisch, S. Ph.D. Thesis, Universität Regensburg, 1989. (f) Fischer, C. Diplomarbeit, Universität Regensburg, 1989. (g) Fischer, C. Ph.D. Thesis, Universität Regensburg, 1991. (h) Daub, J. *Chimia* **1987**, *41*, 52.

(8) (a) Daub, J.; Salbeck, J.; Knöchel, T.; Fischer, C.; Kunkely, H.; Rapp, K. M. *Angew. Chem., Int. Ed. Engl.* **1989**, *28*, 1494. (b) Daub, J.; Fischer, C.; Salbeck, J.; Ulrich, K. *Adv. Mater.* **1990**, *2*, 366. (c) Achatz, J.; Fischer, C.; Salbeck, J.; Daub, J. *J. Chem. Soc., Chem. Commun.* **1991**, 504.

(9) (a) Prinzbach, H.; Herr, H.-J. *Angew. Chem., Int. Ed. Engl.* **1972**, *11*, 135. (b) Prinzbach, H.; Knothe, L. *Pure Appl. Chem.* **1986**, *58*, 25. (c) Laarhoven, W. H. In *Organic Photochemistry*, Padwa, A., Ed.; Dekker: New York, 1987; Vol. 9, p 129.

(10) Görner, H. *J. Photochem. Photobiol. A: Chem.* **1988**, *43*, 263.

(11) (a) Gruen, H.; Görner, H. *J. Phys. Chem.* **1989**, *93*, 7144. (b) Görner, H. *J. Phys. Chem.* **1989**, *93*, 1826. (c) Görner, H.; Fischer, E.; Castel, N. *J. Photochem. Photobiol. A: Chem.* **1990**, *52*, 123.

(12) Heinrich, G.; Schoof, S.; Güsten, H. *J. Photochem.* **1974/75**, *3*, 315.

(13) (a) Hatchard, C. G.; Parker, C. A. *Proc. R. Soc. (London)* **1956**, *A235*, 518. (b) Kuhn, H. J.; Braslavsky, S. E.; Schmidt, R. *Pure Appl. Chem.* **1989**, *61*, 187.

(14) Fischer, G.; Fischer, E. *Mol. Photochem.* **1977**, *8*, 279.

(15) Birks, J. B. *Photophysics of Aromatic Molecules*; Wiley-Interscience: London, 1970.

(16) Carmichael, I.; Hug, G. L. *J. Phys. Chem. Ref. Data* **1986**, *15*, 1.

(17) Whittal, J. In *Photochromism—Molecules and Systems*; Dürr, H., Bouas-Laurent, H., Eds.; Studies in Organic Chemistry, 40; Elsevier: Amsterdam, 1990; p 467.

(18) (a) Saltiel, J.; Sun, Y.-P. In *Photochromism—Molecules and Systems*, ref 4, p 64. (b) Görner, H.; Fischer, E. *J. Photochem. Photobiol. A: Chem.* **1991**, *57*, 235 and references cited therein.

(19) As also pointed out by one reviewer, this proposal is at variance to chemical practice which says that forming covalent bonds tend to have activation energies which are higher than by conformational equilibration by rotation about single bonds. Our assignment is among others based on the experimental finding that in ring-annulated VHF's with sterically fixed *s-cis* structure the thermal back-reaction is significantly faster.<sup>7a</sup> Moreover, acceptor-substituted heptafulvenes and vinylheptafulvenes (see ref 7h) have high dipol moments in the ground state indicating charge displacement to the exocyclic bond and therefore to an increase of the C-8—C-9 bond strength.<sup>24</sup>

(20) Kaftory, M. Technion—Israel Institute of Technology, Haifa, personal communication.

(21) (a) Zimmerman, H. E.; Kamm, K. S.; Werthemann, D. P. *J. Am. Chem. Soc.* **1975**, *97*, 3718. (b) Sugihara, Y.; Wakabayashi, S.; Murata, I.; Jinguji, M.; Nakazawa, T.; Persy, G.; Wirz, J. *J. Am. Chem. Soc.* **1985**, *107*, 5894. (c) Turro, N. J. *Modern Molecular Photochemistry*; Benjamin-Cummings: Menlo Park, CA, 1978; p 170.

(22) (a) Rotkiewicz, K.; Grellmann, K. H.; Grabowski, Z. R. *Chem. Phys. Lett.* **1973**, *19*, 315. (b) Grabowski, Z. R.; Rotkiewicz, K.; Siemiarczuk, A.; Cowley, D. J.; Baumann, W. *Nouv. J. Chim.* **1979**, *3*, 443. (c) Grabowski, Z. R.; Dobkowski, J. *Pure Appl. Chem.* **1983**, *55*, 245.

(23) (a) Rettig, W. *Angew. Chem., Int. Ed. Engl.* **1986**, *25*, 971. (b) Abdel-Mottaleb, M. S. A.; Loutfy, R. O.; Lapouyade, R. *J. Photochem. Photobiol. A: Chem.* **1989**, *48*, 87.

(24) **Note Added in Proof:** Quantum mechanical calculations by semiempirical methods (PM3, UHF formalism) on thermal H-V → H-D isomerization indicate that the ring closure step (*s-cis*-VHF → DHA) is rate determining. Calculated enthalpies of activation are 4.2 and 20.9 kcal/mol for *s-trans*-VHF → *s-cis*-VHF and *s-cis*-VHF → DHA, respectively: Knorr, A. Ph.D. Thesis, Universität Regensburg, in preparation.